CHEMICAL ENGINEERING TRANSACTIONS
VOL. 35, 2013
A publication of AIDIC
The Italian Association of Chemical Engineering
www.aidic.it/cet
Guest Editors: Petar Varbanov, Jiří Klemeš, Panos Seferlis, Athanasios I. Papadopoulos, Spyros Voutetakis

ISBN 978-88-95608-26-6; **ISSN** 1974-9791
DOI: 10.3303/CET1335125

A New Solar Reactor Aperture Mechanism Coupled with Heat Exchanger

Akanksha K. Menon, Asadullah Farid, Nesrin Ozalp*

Texas A&M Univeristy at Qatar , Education City, PO Box 23874, Doha-Qatar
nesrin.ozalp@qatar.tamu.edu

Concentrated solar energy finds applications for power generation and as a source of heat for solar thermochemical processes. However, solar energy reaching the earth's surface is intermittent and fluctuates with weather conditions, position of the sun throughout the day and other seasonal changes. This causes a major drawback in receiver efficiency as semi-constant temperatures are required for efficient operation of solar thermochemical processes. This paper introduces a new variable aperture mechanism which is coupled with a heat exchanger to collect unused heat during peak times. The paper presents an optical and heat transfer analysis of the concept using Monte-Carlo ray tracing technique via TracePro and an in-house developed heat transfer code. The heat transfer analysis of the proposed concept shows the optimum aperture diameter with a compromise between reactor temperature and re-radiation losses. It also predicts the losses incurred by the variable sized aperture mechanism when the incoming solar radiation changes.

1. Introduction

Concentrated solar energy is a sustainable alternative to fossil fuel supported endothermic processes and a viable source of high temperature for solar thermal electricity production (Pitz-Paal et al., 2011). Another very important use of concentrated solar energy is to provide high temperature heat for various solar thermochemical processes, such as solar thermal cracking of natural gas to produce hydrogen and carbon (Ozalp et al., 2010). A special reaction chamber, called "solar reactor", is required to house such solar thermochemical processes. A directly irradiated solar cracking reactor is made of three parts: (1) a cavity, where the reaction takes place, (2) an aperture, where the concentrated solar energy enters through, and (3) inlet and exit ports, for the feedstock and products flow. For an optimum yield, internal cavity temperatures need to be kept constant in order to achieve high overall conversion efficiencies. In this regard, reactor design and configuration plays a significant role to ensure high absorption, multiple internal reflections and minimized losses by radiation (Tescari et al., 2010).

Despite of its many advantages, solar energy is transient in nature, i.e. the solar flux changes depending on the position of the sun throughout the day, lack of sunlight at night and weather fluctuations due to the presence of cloud cover, dust, haze, etc. This results in varying internal temperatures within the solar reactor. Currently, there are two methods widely practiced to control temperature inside solar thermochemical reactors: (1) by changing the flow rate of the feedstock (Saade et al., 2012), (2) by focusing/defocusing heliostats (Sack et al., 2012). Although these are viable solutions to keep internal reactor temperatures constant, flow dynamics is disturbed due to the change in flow rate which would cause problems such as carbon deposition and reactor clogging in solar cracking process (Abanades et al., 2012), and the amount of production yield obtained also varies. Presently, solar reactors use a fixed aperture area for solar radiation to enter the reactor cavity such as those by Maag et al. (2010) with 9 cm diameter aperture, Noglik et al. (2009) with 6 cm, Rodat et al. (2010) with 13 cm, Kogan et al. (2004) with 6.2 cm, and Hirsch and Steinfeld (2004) with 6 cm. However, fixed aperture does not take into account the intermittent nature of solar insolation.

A variable aperture size mechanism was proposed in order to reduce the effects of these problems, where the changes in incoming solar radiation can be tackled via changing the aperture size (Ozalp et al.,

Please cite this article as: Menon A.K., Farid A., Ozalp N., 2013, A new solar reactor aperture mechanism coupled with heat exchanger, Chemical Engineering Transactions, 35, 751-756 DOI:10.3303/CET1335125

2011a). As indicated by Steinfeld and Schubnell (1993) “optimum aperture size results from a compromise between maximizing radiation capture and minimizing radiation losses”. This is mainly because “as we operate at higher and higher temperatures, we seek smaller apertures in order to reduce radiation losses. Contrary to this, larger apertures intercept more sunlight reflected from the concentrators.” Variable aperture size provides an advantage compared to a fixed aperture size by adjusting the area where the flux is intercepted; because the size shrinks during the peak times, the energy that could be used otherwise is lost. In order to decrease the lost energy amount during the peak times due to reducing the aperture size to lessen the radiation losses. The original sliding variable aperture mechanism developed by Ozalp et al. (2011) has been improved and the new concept is presented in this paper which captures the unused solar energy. The new concept involves a much developed variable mechanism which is coupled with a heat exchanger to absorb the excess heat which can be used to preheat feedstock or produce steam. In this paper, the design and manufacturing of the proposed variable aperture coupled with a heat exchanger (HX aperture) is presented. Next, an optical and heat transfer analysis of the concept is presented.

2. Methodology

2.1 Design and Manufacturing

The HX aperture design employs two circular plates – a bottom plate fixed to the reactor body and another plate above it, which is movable. Clockwise rotation of the movable plate creates forces between the arched slots and the protruding shafts of the blades. In turn, the shafts move along the radial slots of the fixed plate. In this manner, instead of the blades moving in a circular fashion, their line of motion is restricted along the radius of the concentric plates. The movable plate is held in the concentric position with four screws. These screws have identical slots to allow sliding of the movable plate.

For the blades to overlap, 24^{o} angled cuts have been made on the sides between the four major blades, and four thinner blades have been introduced to cover up the gaps. Back holders have been created to fit onto the shaft ends to keep the blades intact. For the major blades to carry pipes; each blade has been split into two halves and a semi-circular groove of 7.5 mm is crafted on each one. The pipes used are 6.35 mm in outer diameter, with a safe bend radius of 18.5 mm. The two halves can then be joined together using two 10-24 screws per blade, which sandwich the pipe comfortably. Figure 1 shows the isometric view of the HX aperture assembly created in SolidWorks. The driving force for the rotation will be provided using a drive motor and a dual-link mechanism. Figure 2 shows the aperture concept at minimum opening and the solar reactor with heat exchanger aperture concept mounted on the top flange of the reactor.

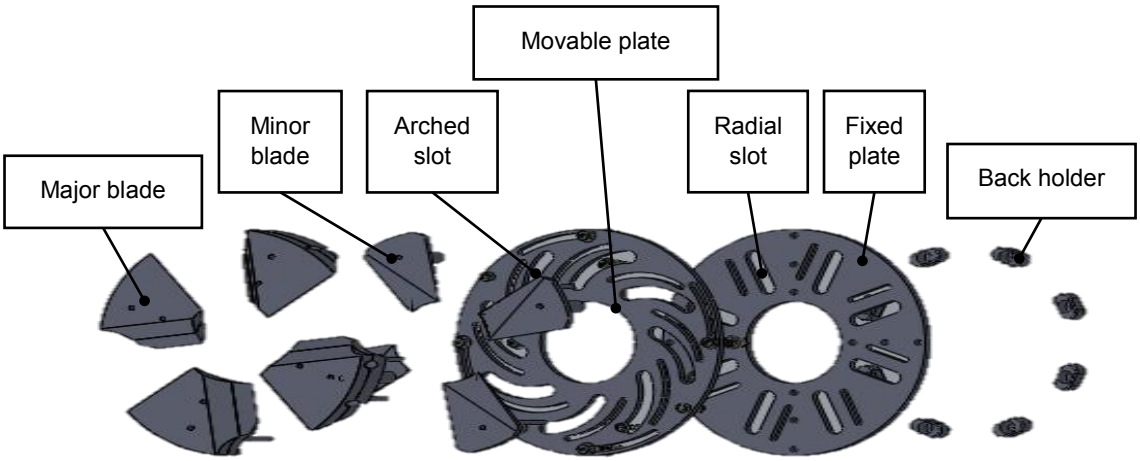

Figure 1: Exploded view of the HX aperture

Figure 2 (a) shows the aperture concept at minimum opening and (b) the solar reactor with heat exchanger aperture concept mounted on the top flange of the reactor. For the blades to overlap, $24°$ angled cuts were made on the sides. In order to cover up the remaining gap between the four major blades, four thinner blades were introduced. To ensure that the blades do not fall off when the aperture is placed vertically, back holders were created to fit onto the shaft ends. For the major blades to carry the tubings, the blade was split into two halves and a semi-circular groove of 7.50 mm crafted on each one. The tubings have

6.35 mm in outer diameter, with a safe bend radius of 18.50 mm. The two halves are joined together using screws, and sandwich the pipe comfortably.

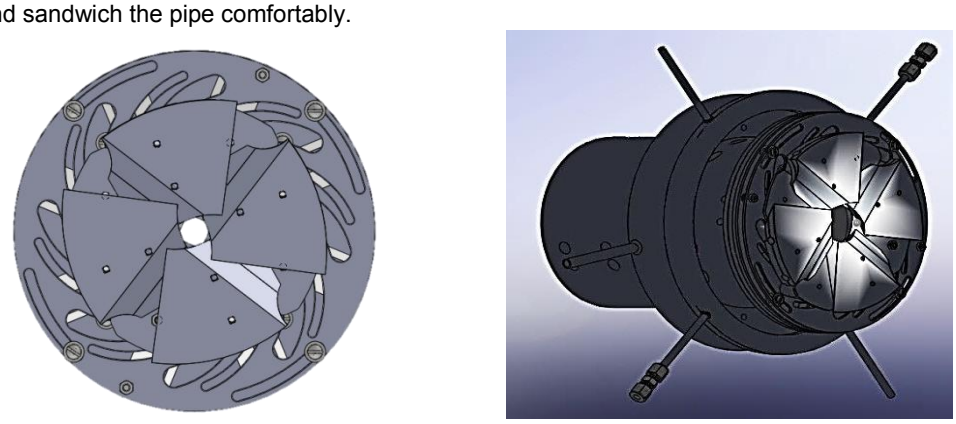

(a) (b)

Figure 2: (a) Aperture at minimum opening, and (b) Solar reactor with variable aperture coupled with a heat exchanger at the top flange

2.2 Optical and Heat Transfer Analysis

Optical and heat transfer analysis was performed to predict the internal reactor temperature when the aperture diameter -and hence its area- is varied. Numerical analysis was done for a 5 kW Xenon-arc lamp (Osram XBO® 5000 W) which can be used as a solar simulator. TracePro commercial software was used to obtain the flux distribution at the focal place using a generalized Monte-Carlo ray tracing (MCRT) technique. The variable aperture mechanism was approximated as a circular opening through which radiation enters. Details of the optical modeling and associated surface properties can be found in Usman et al. (2012). The efficiency of the bulb was assumed to be 60 % and 2 million rays were used for each run with aperture diameters of 20, 60 and 140 mm. TracePro optical analysis was also used to obtain ray information such as the number of primary rays, the direction of incoming rays and the location at which rays intercept the aperture. This information was used as input for the in-house MCRT code developed to obtain the radiation flux and axial temperature distribution within the reactor as explained in detail in (Usman and Ozalp, 2012).

A simplified schematic of the cross-section of the prototype reactor used for the heat transfer analysis is shown in Figure 3. The reactor is divided into sub-systems, namely, cylindrical cavity c_1, front plate *fp*, back plate *bp* and a fluid domain inside the reactor. Cavity c_1 has a length, $L = 175\ mm$, an inner radius, $R_{in} = 70\ mm$ and an outer radius, $R_{out} = 85\ mm$. Cavity c_1 is attached to the front plate *fp* that receives radiation through an aperture of radius R_{ap} mounted in front of it. The front plate is a ring of thickness, $t_{fp} = 5\ mm$, with an inner radius of R_{ap} and outer radius of R_{in}. Cavity c_1 is also attached to a back plate *bp* of thickness, $t_{bp} = 10\ mm$ and outer radius of R_{in}. It has an exit port of radius, $R_{ex} = 5.2\ mm$ through which the working fluid exits the reactor. A ceramic insulation of thickness, $t_{ins} = 5\ cm$ and thermal conductivity, $k_{ins} = 0.1\ W/m.K$ insulates the reactor.

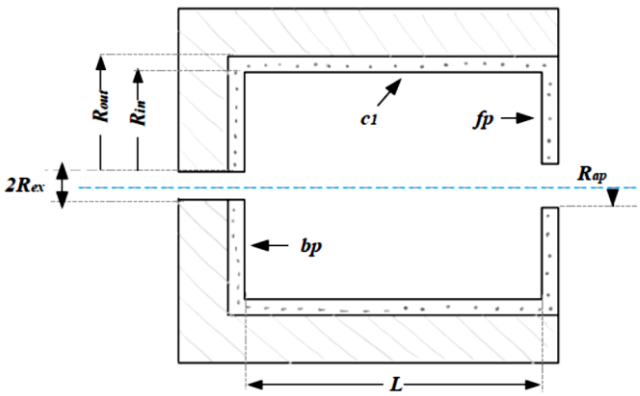

Figure 3: Schematic of reactor cross-section

The cavity c_1 is split into M_1 isothermal ring elements of equal widths, $W_{c1} = L_1/M_1$ and has a corresponding area of $A_{c1} = 2\pi R_{in} W_{c1}$. Similarly, energy conservation equations for the front plate *(fp)* and back plate *(bp)* are obtained using control volume elements as rings of thickness equal to t_{fp} and t_{bp} respectively. The front plate, *fp* is split into M_2 elements of width, $W_{fp} = (R_{in} - R_{ap})/M_2$ and the back plate is split into M_3 elements of width, $W_{bp} = (R_{in} - R_{ex})/M_3$. For an i^{th} element of the front plate and back plate, the corresponding areas are $A_{fp,i} = \pi\, W_{fp}\,(2R_{ap} + 2i\, W_{fp} - W_{fp})$ and $A_{bp,i} = \pi\, W_{bp}\,(2R_{ex} + 2\, i\, W_{bp} - W_{bp})$.
For a preliminary analysis, air was considered as the working fluid. The heat transfer analysis was performed using the same technique described by Usman et al. (2012) including the losses to the surroundings by conduction though the reactor walls and insulation material. For each sub-system, a steady state energy balance was performed to obtain governing equations.
An element, i in cavity c1 receives radiative energy from incoming rays of the solar simulator and also by emissions from other elements of the reactor. A part of the absorbed energy, $Q_{ab,c1,i}$ is re-radiated as emissions, $Q_{em,c1,i}$. Another part is transferred to the adjacent gas phase via convection, $Q_{conv,c1-g,i}$.The rest is lost to the surroundings through conduction through the insulation material and convection to the outside air, $Q_{loss,c1,i}$.The steady-state energy conservation equation for the i^{th} element can be written as,

$$Q_{ab,c1,i} - Q_{em,c1,i} - Q_{conv,c1-g,i} - Q_{loss,c1,i} = 0 \quad (1)$$

The absorption term, $Q_{ab,c1,i}$ is an unknown quantity in Eq(1) and was obtained using Monte-Carlo ray tracing technique. The governing equations were obtained by treating the absorption term and gas temperature as known quantities in Eq(1). Fourth order differential equations for wall temperature were obtained for the cavity and plates.
For the modelling of the fluid domain of air inside cavity c_1, the steady-state energy equation for the control volume is given by:

$$Q_{conv,c1-g,i} - \dot{m}_g c_p (T_{g,i+1} - T_{g,i}) = 0 \quad (2)$$

The inlet gas temperature $T_{g,in}$ was taken as ambient temperature of 300K. This was the boundary condition at the first node, and using Eq(2) the gas temperature for each subsequent node within c_1 was calculated. To solve for unknown reactor temperatures, an initial temperature distribution was assumed for the unknowns: $T_{c,1}$, $T_{fp,i}$, $T_{bp,i}$ and $T_{g,i}$. These initial values were used with the MCRT code to the radiation absorbed by the reactor wall elements. The governing equations were solved simultaneously to obtain the new temperature distribution within the reactor. The values obtained were used as input for MCRT, and this iteration between energy equations and MCRT was continued until an overall energy balance criterion is satisfied, as described in Usman et al. (2012).
To imitate the changing solar flux throughout the day, data for direct normal radiation from the sun was obtained from the National Renewable Energy Laboratory (NREL, 2011). The irradiance value at 04:49 h, 08:00 h and 12:31 h were chosen and the corresponding power intercepted by a 20 mm, 60 mm and 140 mm aperture diameters were calculated. The values were scaled down to the range of the aforementioned 5 kW solar simulator and obtained as 1 kW at 04:49 h, 3.5 kW at 08:00 h and 5 kW at 12:31 h that imitates the position of the sun from morning to noon. These fluxes were then adjusted to accommodate for the 60 % efficiency of the bulb used. Distribution of the power intercepted and the losses were numerically calculated using the in-house MATLAB® code for aperture diameters of 20 mm and 60 mm.

3. Results

3.1 Optics and Heat Transfer Analysis

The theoretical performance of the system was obtained from flux maps using a 5 kW solar simulator. Gaussian flux distribution was obtained which peaks at the centre and diminishes to zero. The heat transfer efficiency, defined as the amount of radiative energy originating at the source that reaches the target, was determined to be 45.63 %. Table 1 shows the reactor wall and gas temperature obtained from the numerical analysis for variable apertures corresponding to incoming power of 3 kW.
The average gas temperature is 647 K at a 60 mm diameter aperture and drops to 450 K for a 140 mm aperture. This is because for a larger aperture diameter, re-radiation losses dominate due to the fourth power dependence on temperature. It is seen that there is a compromise between the power intercepted and the corresponding re-radiation losses, with 60 mm being the optimum aperture diameter in this particular case.

Table 1: Numerically simulated reactor wall and gas temperature

Aperture diameter (mm)	Average gas temperature (K)	Reactor wall temperature (K)
20	393	489
60	647	822
140	450	591

Based on the solar power levels provided in NREL data from morning to noon which were scaled in accordance to the power levels of the aforementioned 5 kW solar simulator, the distribution of intercepted power for a small aperture diameter of 20 mm and the optimum one of 60 mm were obtained as shown in Table 2.

Table 2: Distribution of power intercepted at the aperture from morning to noon

Diameter (mm)	Intercepted at aperture (W)	Transferred to working fluid (W)	Re-radiation from aperture (W)	Escaping through exit port (W)	Lost by conduction (W)
Incoming power = 600 W (0449 hrs)					
20	39.29	9.57	2.63	1.01	26.08
60	206.14	35.57	77.49	5.83	87.25
Incoming power = 2.1 kW (0800 hrs)					
20	142.18	34.61	10.21	3.82	93.54
60	721.5	128.49	329.68	22.46	240.87
Incoming power = 3 kW (1231 hrs)					
20	198.65	52.65	12.95	5.13	127.91
60	1030.68	171.58	475.89	31.8	351.42

4. Conclusions

A new aperture concept of a variable aperture coupled with a heat exchanger (HX aperture) was presented. This concept offers promising results towards maintaining semi-constant temperatures inside a solar reactor under varying incoming solar flux and provides an option to use the excess heat to preheat the feedstock or generate steam for low temperature processes. An optical and heat transfer analysis of the concept was performed using Monte-Carlo ray tracing coupled with a steady-state energy solver for numerical analysis. The average gas temperature was found to be 647 K at a 60 mm diameter aperture, making this the optimum aperture diameter.

Acknowledgement

This research has been funded by National Priorities Research Program of Qatar National Research Fund (QNRF) Project No: NPRP 09 – 670 – 2 – 254.

References

Abanades A., Rubbia C., Salmieri D., 2012. Technological challenges for industrial development of hydrogen production based on methane cracking, Energy, 46, 359-363.

Hirsch D., Steinfeld A., 2004. Solar hydrogen production by thermal decomposition of natural gas using a vortex-flow reactor, International Journal of Hydrogen Energy, 29, 47-55.

Kogan A., Kogan M., Barak S., 2004. Production of hydrogen and carbon by solar thermal methane splitting. II. Room temperature simulation tests of seeded solar reactor. International Journal of Hydrogen Energy, 29, 1227-1236.

Maag G., Rodat S., Flamant G., Steinfeld A., 2010. Heat transfer model and scale-up of an entrained-flow solar reactor for the thermal decomposition of methane, International Journal of Hydrogen Energy, 35(24), 13232-13241.

NREL (National Renewable Energy Laboratory), 2011, NREL Database. <www.nrel.gov/midc/srrl_rsp2>, Accessed 05/01/2013.

Noglik A., Roeb M., Sattler C., Pitz-Paal R., 2009. Experimental study on sulphur trioxide decomposition in a solar receiver-reactor, Int. J. En. Res., 33, 799-812.

Ozalp N., Epstein M., Kogan A., 2010, Cleaner pathways of hydrogen, carbon nano-materials and metals production via solar thermal processing, Journal of Cleaner Production, 18(9), 900-907.
Ozalp N., Toyama A., Mohamed T., Al Shammasi M., Roshan D., Farghaly A., 2011. A smart solar reactor for environmentally clean chemical processing, Chemical Engineering Transactions, 25, 989-994.
Pitz-Paal R., Botero N.B., Steinfeld A., 2011. Heliostat field layout optimization for high-temperature solar thermochemical processing, Sol. En., 85, 334-343.
Rodat S., Abanades S., Flamant G., Sana J., 2010. A pilot-scale solar reactor for the production of hydrogen and carbon black from methane splitting, International Journal of Hydrogen Energy, 35, 7748-7758.
Saade E., Bingham C., Clough D.E., Weimer A., 2012. Dynamics of a solar-thermal transport-tube reactor. Chemical Engineering Journal, 213, 272-285.
Sack J.P., Roeb M., Sattler C., Pitz-Paal R., Heinzel A., 2012. Development of a system model for a hydrogen production process on a solar tower, Sol. En., 86, 99-111.
Steinfeld A., Schubnell M., 1993. Optimum aperture size and operating temperature of a solar cavity-receiver, Sol. En., 50(1), 19-25.
Tescari S., Mazet N., Neveu P., 2010. Constructal method to optimize solar thermochemical reactor design, Sol. En., 84(9), 1555-1566.
Usman S., Ozalp N., 2012, Numerical and optical analysis of a weather adaptable solar reactor. 9th International Conference on Heat Transfer, Fluid Mechanics and Thermodynamics (HEFAT 2012), Malta, 16-18 July 2012, Paper ID: 1569576105.
Usman S., Saleem A., Menon A., Ozalp, N., 2012, Experimental testing of a variable aperture concept for solar thermochemical reactors. SolarPACES conference, Marrakech, Morocco, September 11-14, 2012, Paper ID: 46576.